Kinetic plasticity and the determination of product ratios for kinetic schemes leading to multiple products without rate laws — New methods based on directed graphs

John Andraos

Abstract: This paper presents two new and fast methods of determining product ratios for kinetic schemes leading to more than one product on which the Acree–Curtin–Hammett (ACH) principle is based. The methods involve rewriting a given kinetic scheme as a directed graph with nodes and arrows connecting the nodes and takes advantage of the directionality of the kinetic arrows and the enumeration of paths to the various target product nodes. The first, based on path divergent trees, is computationally simpler but works under a specific set of conditions, whereas the second, based on an adapted version of Chou's graphical method, works for all cases. By means of illustrated examples, both methods are shown to be completely verifiable with conventional more tedious treatments based on rate law determinations. The directed graph concept also works for kinetic schemes that involve entirely equilibrated species. In addition, the paper extends these ideas to variants of the basic ACH scheme, thereby testing the validity of the ACH principle and bringing about a deeper understanding of it. Generalization of the results yields a new parameter, called degree of kinetic plasticity, which completely describes the dynamics of kinetic resolution between the boundary limits of ACH behaviour (100% kinetic plasticity) and anti-ACH behaviour (100% kinetic rigidity). It is shown that this parameter is a good descriptor of all possible scenarios between and including these limits and can be determined experimentally by conducting a new kind of product study that tracks the behaviour of final product excesses as a function of initial substrate excesses. The resulting plot is always linear with a positive slope. The degree of kinetic plasticity is found by simply subtracting the slope from unity. These ideas are tested on complex kinetic schemes exhibiting dynamic kinetic resolution (DKR) by means of organocatalysis.

Key words: physical organic chemistry, kinetics, mechanism, directed graph, Chou digraph, Chou graphical rule, Acree-Curtin-Hammett principle, product ratio, dynamic kinetic resolution, organocatalysis.

Résumé : Dans ce travail on a développé deux nouvelles méthodes rapides pour déterminer les rapports des schémas conduisant à plus d'un produit sur lequel se base le principe d'Acree–Curtin–Hammett (ACH). Les méthodes impliquent une réécriture d'un schéma cinétique donné sous la forme d'un graphique dirigé comportant des nodes et des flèches reliant les nodes et elles tirent avantage du caractère directionnel des flèches cinétiques et de l'énumération des voies vers les divers nodes des produits prévus. La première, qui est basée sur des ramifications divergentes, est la plus simple d'un point de vue des calculs théoriques, mais elle ne s'applique que dans un ensemble spécifique de conditions alors que la deuxième qui est basée sur une version adaptée de la méthode graphique de Chou s'applique à tous les cas. En faisant appel à des illustrations appropriées, on peut démontrer que les deux méthodes peuvent être entièrement vérifier à l'aide de traitements conventionnels plus fastidieux basés sur des déterminations de lois de vitesses. Le concept du graphique dirigé fonctionne aussi pour les schémas cinétiques qui impliquent des espèces entièrement équilibrées. De plus, ce travail permet d'élargir ces idées à des variantes du schéma de base de Acree-Curtin-Hammett qui permet ainsi de vérifier la validité du principe d'ACH et de mieux la comprendre. La généralisation des résultats conduit à un nouveau paramètre, le degré de plasticité cinétique, qui décrit complètement la dynamique de la résolution cinétique entre les limites de la frontière entre le comportement Acree-Curtin-Hammett (100% de plasticité cinétique) et le comportement anti-Acree–Curtin–Hammett (100% de rigidité cinétique). On a montré que ce paramètre permet de bien décrire tous les scénarios entre, et incluant, ces limites et qu'il peut être déterminé expérimentalement en effectuant un nouveau type d'étude de produit qui permet de suivre le comportement des excès de produit final en fonction d'excès de substrats initiaux. La courbe qui en résulte est toujours linéaire avec une pente positive. On détermine le degré de plasticité cinétique en soustrayant la pente de l'unité. On a fait appel à l'organocatalyse pour tester ces idées sur les schémas cinétiques complexes qui présentent de la résolution cinétique dynamique (RCD).

This paper is dedicated to the memory of Keith Yates.

J. Andraos. Department of Chemistry, York University, Toronto, ON M3J 1P3, Canada (e-mail: jandraos@yorku.ca).

doi:10.1139/V08-020

[Traduit par la Rédaction]

Introduction

The Acree–Curtin–Hammett (ACH) principle is a fundamental concept in mechanistic chemistry that has been used to approximate under simplifying conditions the magnitude of the final product ratio for a pair of products originating from a pair of equilibrating starting materials as shown in Scheme 1. The starting materials may be equilibrating conformers, tautomers, or stereoisomers. Curtin and Hammett demonstrated this principle in the 1950s for products arising from equilibrating conformers (1, 2); however, it had already been described much earlier by Acree in 1907 for products arising from equilibrating tautomers (3). Moreover, Acree's work also derived what would be later known as the Winstein–Holness equation (4). A recent report has described the connections between these works and brought Acree's forgotten work to light (5). Throughout this paper, the principle is therefore referred to as the ACH principle or kinetic theorem to recognize the contributions of the three scientists. It is a concept that is well discussed in several textbooks of mechanistic organic chemistry (6–8), a review (9), and a pedagogical article (10).

Simply stated, the final product ratio $[P_X]:[P_Y]$ is equal to the ratio of product forming rate constants $k_3:k_4$ if the magnitudes of the rate constants k_1 and k_2 involved in the equilibration between X and Y are similar and are very large compared with those of the product forming steps. This independence of the final product ratio on the dynamics of the preceding equilibrium and the amounts of starting materials defines the ACH condition and is a direct result of applying *both* kinetic conditions. When these conditions are not met, an exact analytical solution to the above kinetic scheme becomes necessary to determine the complete form of the final product ratio. Equation [1] yields the complete dependence of the final product ratio on all four rate constants and the starting amounts of X and Y (11).

[1] $$\frac{[P_X]_\infty}{[P_Y]_\infty} = \left(\frac{k_3}{k_4}\right)\left[\frac{(a+b)\,k_2 + ak_4}{(a+b)\,k_1 + bk_3}\right]$$

where a and b represent the initial amounts of X and Y at time zero. It is easy to verify that the right-hand side of eq. [1] reduces to k_3/k_4 when (*i*) k_1 and $k_2 \gg k_3$ and k_4 and (*ii*) $k_1 = k_2$. Note that if only condition (*i*) holds, then the final product ratio will have a dependence on both the ratio k_3/k_4 and the equilibrium constant $K = k_1/k_2$, according to eq. [2].

[2] $$\frac{[P_X]_\infty}{[P_Y]_\infty} = \left(\frac{k_3}{k_4}\right)\left(\frac{1}{K}\right)$$

In addition to applying to equilibrating conformers or tautomers, the kinetic scheme shown in Scheme 1 is applicable to the technique of dynamic kinetic resolution (DKR) (12–38) used in synthetic organic chemistry to optimize the synthesis of stereoisomeric products from corresponding enantiomeric or diastereomeric starting materials that are in equilibrium. This is arguably the most important practical application of the ACH principle. In fact, it is this special phenomenon that blends the interests of both mechanistic and synthetic organic chemists. Mechanistic chemists are attracted to reactions that yield multiple products via multiple intermediates but that have the potential to be perturbed to produce one target product under the "right" set of conditions once their corresponding mechanism landscapes are completely elucidated. Synthetic chemists are of course interested in reactions that yield only one target product in high yield and high regio-, stereo-, and chemo-selectivity. Scheme 2 shows an analogous kinetic system to that in Scheme 1 with appropriate stereochemical descriptors R and S for substrates and products.

If a chemical reaction produces enantiomeric or diastereomeric products, and it is desired to carry out a subsequent transformation on one of them, then one is faced with the prospect of first separating or resolving the product mixture from the first reaction, usually racemic, before carrying out the second. Resolution of racemic mixtures by standard methods results in an automatic loss of half the starting material, assuming that the resolution procedure goes to completion. This means that if the individual stereoisomers in the starting racemic mixture are not interconvertible then the maximum amount of desired product formed in the subsequent step is exactly half that of the starting material, and so the maximum yield for this second step is 50%. This situation is designated as anti-ACH behaviour and corresponds to kinetic resolution. If, on the other hand, there is a possibility to have a rapid interchange between starting materials via a racemization process to an extent that the ACH condition applies, then in principle it is possible to shunt all of the starting material toward the product of interest in the subsequent reaction. The more dynamic the equilibration is between S_R and S_S, the more likely this outcome will occur. This situation is designated as ACH behaviour and corresponds to dynamic kinetic resolution.
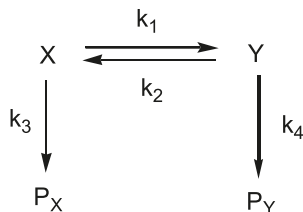
In a recent report published in 2003, the complete dynamics of Scheme 2 was explored including a full kinetic analysis of the dependence of the initial and final product ratios on all four rate constants and starting amounts of S_R and S_S (11). The method used to derive expressions for these ratios shown in eqs. [3] and [4],

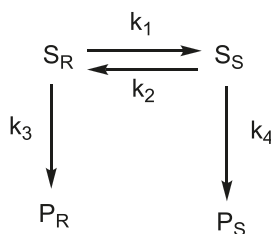[3] $$\frac{[P_R]_0}{[P_S]_0} = \left(\frac{a}{b}\right)\left(\frac{k_3}{k_4}\right)$$

[4] $$\frac{[P_R]_\infty}{[P_S]_\infty} = \left(\frac{k_3}{k_4}\right)\left[\frac{(a+b)\,k_2 + ak_4}{(a+b)\,k_1 + bk_3}\right]$$

where a and b are the initial amounts of S_R and S_S respectively, was the method of Laplace transforms (39). It is important to point out that though there are no products formed initially their ratio extrapolated to zero time is in fact a finite

Scheme 1.

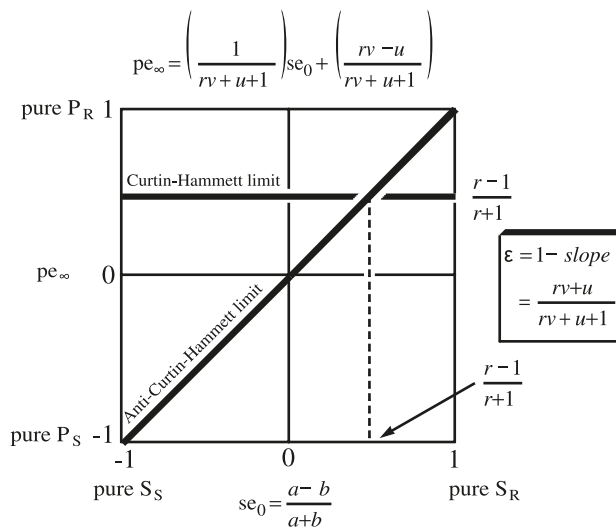$$X \underset{k_2}{\overset{k_1}{\rightleftharpoons}} Y$$

$$X \xrightarrow{k_3} P_X \qquad Y \xrightarrow{k_4} P_Y$$

Scheme 2.

$$S_R \underset{k_2}{\overset{k_1}{\rightleftharpoons}} S_S$$

$$S_R \xrightarrow{k_3} P_R \qquad S_S \xrightarrow{k_4} P_S$$

Fig. 1. Relationship between final product excess and initial substrate excess according to eq. [8], showing the two limiting slopes corresponding to the Curtin–Hammett condition (zero slope, u and $v \rightarrow 0$, 100% kinetic plasticity) and anti-Curtin–Hammett condition (unit slope, u and $v \rightarrow \infty$, 0% kinetic plasticity or 100% kinetic rigidity).

$$pe_\infty = \left(\frac{1}{rv+u+1} \right) se_0 + \left(\frac{rv-u}{rv+u+1} \right)$$

quantity. This observation is entirely consistent with the work of Noyori and co-workers (40, 41) who showed plots of % final enantiomeric excess of product versus % conversion that had well-defined nonzero intercepts. The two expressions given in eqs. [3] and [4] suggested a new kind of experiment that could be carried out that would quantitatively determine the intrinsic efficiency or plasticity of dynamic kinetic resolution that depended only on key rate constant ratios. This parameter was shown to be able to account for all experimentally observed cases between and including the limits of complete dynamic kinetic resolution (ACH conditions) and complete kinetic resolution (anti-ACH conditions) for simple kinetic schemes such as that shown in Scheme 2.

The crux of the new experiment is to determine initial and final product ratios for a *set* of initial substrate ratios covering the full range of possible optical purities of starting materials beyond the simple racemic condition, which is the universal initial composition of starting materials. Hence for a given starting substrate ratio a/b, one records time-dependent product progress curves, and from these the initial and final product ratios are determined by extrapolation to zero and infinite times. A plot of $[P_R]_0/[P_S]_0$ vs. a/b yields a slope equal to $r = k_3/k_4$. A plot of final product excess with respect to P_R and pe_∞ vs. initial substrate excess with respect to S_R and $(a–b)/(a+b)$, according to eq. [5],

$$[5] \qquad pe_\infty = \frac{[P_R]_\infty - [P_S]_\infty}{[P_R]_\infty + [P_S]_\infty} = \frac{\dfrac{[P_R]_\infty}{[P_S]_\infty} - 1}{\dfrac{[P_R]_\infty}{[P_S]_\infty} + 1}$$

$$= \frac{1}{rv+u+1} \left(\frac{a-b}{a+b} \right) + \frac{rv-u}{rv+u+1}$$

yields a slope equal to $1/(rv + u + 1)$ and an intercept equal to $(rv – u)/(rv + u + 1)$ where $r = k_3/k_4$, $u = k_1/k_3$, and $v = k_2/k_3$. The rate constant ratios u and v may be determined directly from the slope and intercept of such a plot using eqs. [6] and [7],

$$[6] \qquad u = \frac{1}{2} \left[\frac{1 - \text{intercept}}{\text{slope}} - 1 \right]$$

and

$$[7] \qquad v = \frac{1}{2r} \left[\frac{1 + \text{intercept}}{\text{slope}} - 1 \right]$$

An expression for the intrinsic efficiency or degree of kinetic plasticity of dynamic kinetic resolution, ε_{DKR}, may be obtained by examining the full range of possible values for the slope of this plot. In the ACH limit where $u = v \rightarrow \infty$ so that $k_1 = k_2$ and $k_1, k_2 \gg k_3, k_4$, the slope reaches a minimum value of zero. This result indicates that the final product ratio is independent of the starting amounts of S_R and S_S. In the anti-ACH limit where $u = v = 0$ so that $k_1 = k_2$ and $k_1, k_2 \ll k_3, k_4$, the slope reaches a maximum value of one. This case indicates that the final product ratio mirrors the initial starting material ratio. From these two boundary conditions, we set $\varepsilon_{DKR} = 1$ to represent the ACH case of 100% efficiency or complete kinetic plasticity and $\varepsilon_{DKR} = 0$ to represent the anti-ACH case of 0% efficiency or complete kinetic rigidity. Hence, we may define the intrinsic efficiency or performance of dynamic kinetic resolution as in eq. [8] to describe the pliability of the equilibrium toward being pulled in either direction by either of the product forming steps.

$$[8] \qquad \varepsilon_{DKR} = 1 - \text{slope} = 1 - \frac{1}{rv+u+1} = \frac{rv+u}{rv+u+1}$$

Figure 1 illustrates graphically the two limiting cases described earlier. Equation [5] predicts that experimental data should obey a linear relationship with a positive slope falling between these two limits. The intersection of the two limiting lines suggests that there exists a unique combination of initial substrate amounts that will result in the same final

product ratio, and hence the same final product excess, under both limiting conditions. It should be noted that eq. [5] also predicts that we can never have a plot with a slope of zero and an intercept of zero, i.e., a line falling along the x-axis. Such a condition would correspond to the nonsense situation of a completely plastic kinetic system that begins with any combination of substrates and always ends up with a racemic mixture of products. Setting the slope and intercept to be simultaneously zero in eq. [5] leads to a contradiction in the allowable domains of the parameters u and v, namely, $u, v \to \infty$ for the slope and $u, v \to 0$ for the intercept. A racemic mixture of products can only arise from a racemic mixture of starting materials, which immediately suggests that the kinetic system is 100% rigid and hence the anti-ACH limiting line of unit slope and zero intercept is operative. However, ACH limiting lines with zero slopes and intercepts of +1 or –1 are allowed, i.e., lines falling along the top and bottom edges of the square in Fig. 1. These correspond to the fully dynamic situations where the equilibrium step is fast compared with the product forming steps ($u, v \to \infty$) and $r \to \infty$ (or $k_3 \ggg k_4$) for the case of an intercept of +1, and $r \to 0$ (or $k_3 \lll k_4$) for the case of an intercept of –1. From Scheme 2, the former case essentially corresponds to the case when the step from S_S to P_S is shut down so that the only product formed is P_R, and the latter case corresponds to the opposite situation when the step from S_R to P_R is shut down so that the only product formed is P_S. The plot shown in Fig. 1 may be used as a diagnostic test to verify if a given chemical system obeys ACH kinetic-type schemes.

Equation [8] is applicable to any kinetic scheme that looks like Scheme 1 or 2 regardless of the isomeric relationship of the starting materials so long as their starting ratio is controllable. In the case of isomeric substrates that cannot be easily separated and their initial ratio manipulated as described above, separate kinetic experiments are required to determine individual rate constants so that the kinetic plasticity parameter given in eq. [8] may be determined. To date there has not yet been any experimental verification of this new idea reported in the literature. However, the 2003 report did survey a number of published chemical systems where enough experimental detail was given so that minimum estimates of ε_{DKR} could be made, and thus the validity of eq. [8] was confirmed in principle. In that work, several variant kinetic schemes were examined and their properties and corresponding exact initial and final product ratio expressions were derived. The important point gleaned from that investigation was that all prior work on such kinetic systems *assumed* from the outset that the ACH condition was valid and that Winstein–Holness kinetic behaviour (4) was applicable. These claims were then verified by carrying out *independent* theoretical calculations to determine energy barriers pertaining to the relevant transition states (42). The above analysis clearly shows that the ACH condition may be verified directly from wholly experimentally acquired data without need for further computation. Moreover, even if it turns out that this special condition may not be met for a given chemical system it is still possible to quantify the actual extent of meeting this condition according to the parameter defined in eq. [8].

Having introduced the current understanding of the ACH principle on simple kinetic systems, we now report on fur-

Scheme 3.
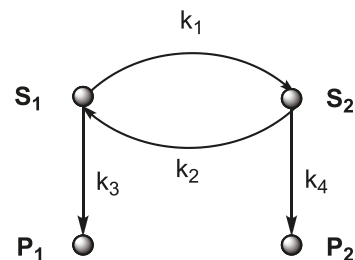
ther extensions that test the validity of this principle on complex kinetic systems. Extended linear and cyclic kinetic schemes are examined in detail. The concept of kinetic plasticity described above is generalized and the statement of the ACH principle is revised accordingly. In doing so, we also introduce two new time-saving methods of determining the required product ratio expressions for initial and final reaction times that serves as a check for conventional treatments, namely, the Laplace transform method. As a bonus, it will be demonstrated that they also circumvent much of the tedious computation that is a consequence of handling complex kinetic systems. Limitations of the methods are also discussed.

Directed graph method

In this section we introduce easy-to-use algorithms for determining expressions as shown in eqs. [1] and [4], without the use of rate laws. The methods are based on directed graphs, or digraphs (43), and are applicable to competitive-type kinetic schemes leading to multiple products from one or more substrates. The schematic method of King and Altman described in 1956 is a forerunner report describing the use of graphs to derive rate laws for enzyme-catalyzed reactions (44). Chou has previously described powerful algorithms for analyzing non-steady-state and steady-state enzyme kinetics and protein folding kinetics (45–61).
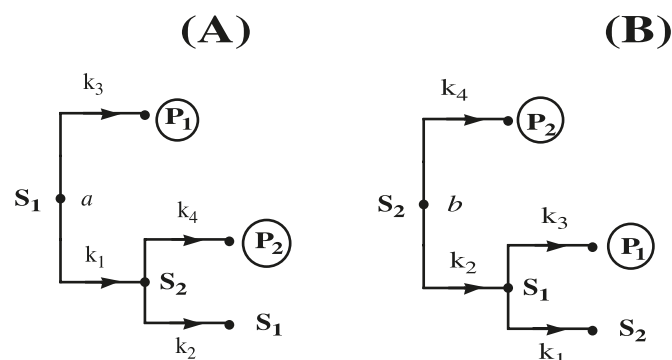
Digraphs are objects that consist of a finite set of vertices and a set of ordered pairs of distinct vertices called arcs. If the ordered pair $\{x, y\}$ is an arc, then the arc is said is to be directed from x to y. The kinetic schemes shown in Schemes 1 and 2 may be immediately drawn as digraphs, since the chemical entities and reaction arrows are translated as vertices and arcs, respectively, according to the above definitions (see Scheme 3).

The substrate vertices are designated as source nodes and the product vertices as sink nodes. The arrows and rate constant descriptors are retained as before in the usual sense. For the first method based on path divergent trees, beginning with each source node we draw a corresponding divergent tree that enumerates all paths from that node to all product nodes. In doing so, we apply the following rules. For irreversible steps one stops when a product node is reached and for reversible steps one stops when a previously traversed node along that branch is reached. Hence, we have for Scheme 3 the two divergent trees shown in Fig. 2 in which we assign the initial condition that we begin with amounts a and b for substrates S_1 and S_2.

Next, we write expressions for the expected contribution of each product based on the attenuation of the initial amounts of each source node that lead to each product. This

Fig. 2. Path divergent trees for paths emanating from S1 (A) and S2 (B). See Scheme 3.

$$[11] \quad \frac{[P_1]_\infty}{[P_2]_\infty} = \frac{\left(\dfrac{k_3}{k_1 + k_3}\right)\left[a + b\left(\dfrac{k_2}{k_2 + k_4}\right)\right]}{\left(\dfrac{k_4}{k_2 + k_4}\right)\left[b + a\left(\dfrac{k_1}{k_1 + k_3}\right)\right]}$$

$$= \left(\frac{k_3}{k_4}\right)\left[\frac{(a + b)k_2 + ak_4}{(a + b)k_1 + bk_3}\right]$$

which is identical to eqs. [1] and [4]. The initial product ratio is also given directly by eq. [12],

$$[12] \quad \frac{[P_1]_o}{[P_2]_o} = \frac{ak_3}{bk_4}$$

which is identical to eq. [3]. Note that in eq. [12] the numerator refers to the shortest path from S_1 to P_1 and the denominator refers to the shortest path from S_2 to P_2. This observation turns out to be always true in the determination of expressions for initial product ratios by the digraph method.

It is obvious how facile this method is compared with the standard method of Laplace transforms (39) that becomes more tedious as the number of substrate and product nodes increase and the number of rate constant connections between them increases. It may be recalled that the Laplace transform method involves taking determinants of square matrices whose dimension is equal to the sum of the number of substrates, intermediates, and products involved in the kinetic scheme. In addition, the method relies on tables of inverse transforms that need to be worked out separately, but such tables are readily available (62–64). A key limitation of the method is that it is applicable only to unimolecular or pseudo-unimolecular kinetic systems and not biomolecular ones, since the Laplace transform of a product of functions is not equal to the product of their Laplace transform functions as shown in eq. [13],
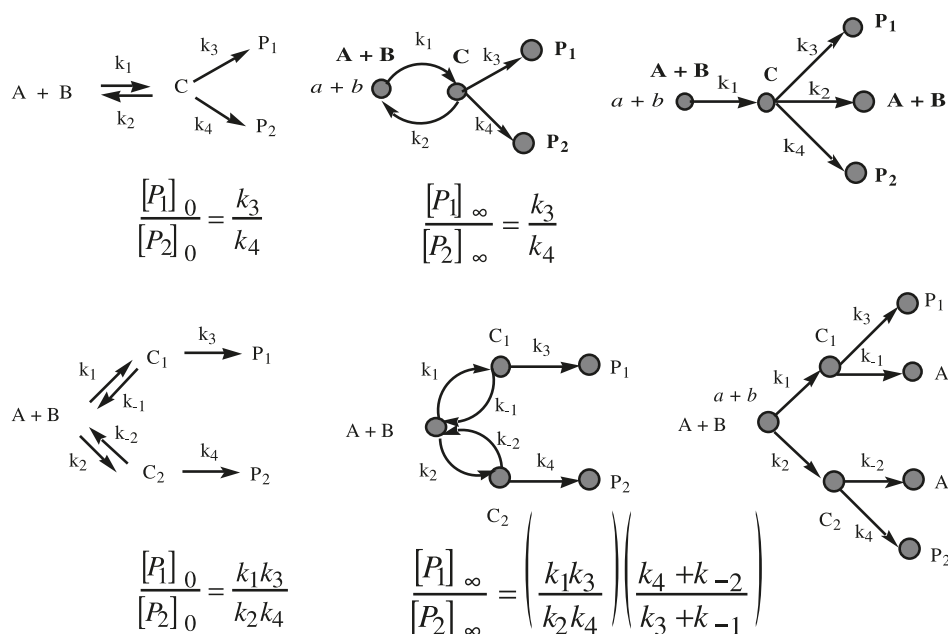
$$[13] \quad L\{f(t) \bullet g(t)\} \neq L\{f(t)\} \bullet L\{g(t)\}$$

Figure 3 summarizes key definitions and the sequence of steps involved in this method. For illustration and comparison with the directed graph method, the Supplementary Data contains a full solution of the kinetic scheme shown in Scheme 3 by the Laplace transform method.[2]
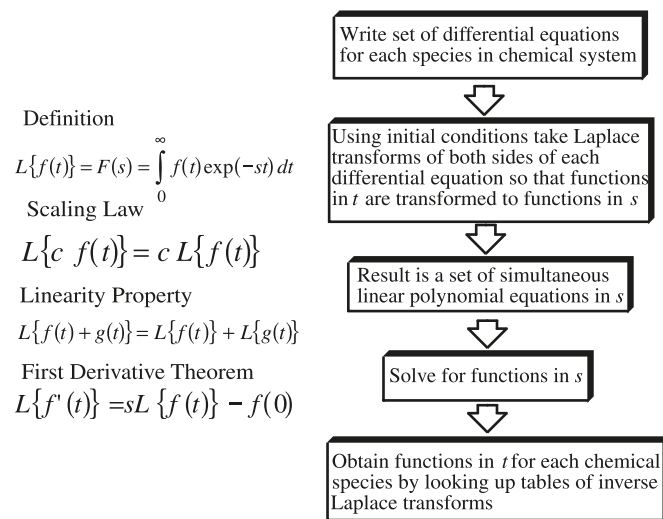
For verification purposes, all of the expressions for initial and final product ratios derived previously (11) were confirmed by the new digraph method. These are also given in the Supplementary Data.[2] Reassuringly, this consistency demonstrates that the present new method also serves as an excellent checking device. However, this method does have its limitations. First, it does not give analytical expressions for the time-dependent substrate and product concentration profiles. For the purposes of determining analytical expressions for product ratios at the beginning and at the end of reactions, paradoxically these are not necessary. Second, like

is done following the connectivities between nodes in the path divergent trees. Thus, for paths leading to product P_1 we have eq. [9],

$$[9] \quad a\left(\frac{k_3}{k_1 + k_3}\right) + b\left(\frac{k_3}{k_1 + k_3}\right)\left(\frac{k_2}{k_2 + k_4}\right)$$

$$= \left(\frac{k_3}{k_1 + k_3}\right)\left[a + b\left(\frac{k_2}{k_2 + k_4}\right)\right]$$

The first term in eq. [9] pertains to P_1 originating directly from S_1 along the k_3 branch (see Fig. 2A). Note that since there are two branches emanating from S_1, the fraction of starting material a leading to P_1 is $k_3/(k_3 + k_1)$. The second term pertains to P_1 originating from S_1, which in turn originated from S_2 (see Fig. 2B). The starting amount of S_2, b, is first split along the k_2 branch and then is split again along the k_3 branch. Hence, we have the corresponding multiplication of fractions.

Similarly, we have for paths leading to product P_2

$$[10] \quad b\left(\frac{k_4}{k_2 + k_4}\right) + a\left(\frac{k_1}{k_1 + k_3}\right)\left(\frac{k_4}{k_2 + k_4}\right)$$

$$= \left(\frac{k_4}{k_2 + k_4}\right)\left[b + a\left(\frac{k_1}{k_1 + k_3}\right)\right]$$

Note that since we have a symmetrical digraph, the pairs of subscripts a and b, 1 and 3, and 2 and 4, are interchangeable in both expressions. This implies that the expression in eq. [10] could have been written at once from eq. [9] using these variable interchanges.

The final product ratio is then given directly by dividing eq. [9] by eq. [10] thus yielding eq. [11],

Fig. 4. Example special bimolecular kinetic systems whose initial and final product ratios are determinable exactly by the directed graph method based on path divergent trees.


$$\frac{[P_1]_0}{[P_2]_0} = \frac{k_3}{k_4}$$

$$\frac{[P_1]_\infty}{[P_2]_\infty} = \frac{k_3}{k_4}$$

$$\frac{[P_1]_0}{[P_2]_0} = \frac{k_1 k_3}{k_2 k_4}$$

$$\frac{[P_1]_\infty}{[P_2]_\infty} = \left(\frac{k_1 k_3}{k_2 k_4}\right)\left(\frac{k_4 + k_{-2}}{k_3 + k_{-1}}\right)$$

Fig. 3. Key definitions and sequence of steps involved in the Laplace transform method.

Definition

$$L\{f(t)\} = F(s) = \int_0^\infty f(t)\exp(-st)\,dt$$

Scaling Law

$$L\{c\ f(t)\} = c\ L\{f(t)\}$$

Linearity Property

$$L\{f(t) + g(t)\} = L\{f(t)\} + L\{g(t)\}$$

First Derivative Theorem

$$L\{f'(t)\} = sL\{f(t)\} - f(0)$$

Write set of differential equations for each species in chemical system

⇩

Using initial conditions take Laplace transforms of both sides of each differential equation so that functions in t are transformed to functions in s

⇩

Result is a set of simultaneous linear polynomial equations in s

⇩

Solve for functions in s

⇩

Obtain functions in t for each chemical species by looking up tables of inverse Laplace transforms

the Laplace transform method, it is applicable to unimolecular and pseudo-unimolecular kinetic systems. However, it can still be applied to special bimolecular systems, such as those shown in Fig. 4 where multiple products arise from a common intermediate via unimolecular steps though that intermediate itself arose from a prior bimolecular step. For these few examples, though time-dependent concentration profiles for products cannot be determined analytically, their product ratios are determinable exactly by the directed graph method.

A key observation from the path divergent trees shown in Fig. 2 is that each tree is composed of two stages or tiers with only one repeat node. For Fig. 2*A* the repeat node is S1 and for Fig. 2*B* it is S2. It turns out that if the construction of path divergent trees from a digraph pertaining to a kinetic

Scheme 4.
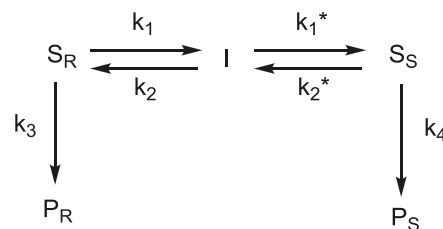
scheme according to the above algorithm leads to trees having more than one repeat node appearing in *different* stages, then the above digraph method does not yield expressions for the product ratio that are consistent with those obtained from the check Laplace transform method. Extra terms appear in the numerator and the denominator for the final product ratio expression, which ultimately yield an apparent dependency on the amounts of equilibrating starting materials when the ACH condition is applied. This would lead to the erroneous conclusion that the ACH principle is violated for such cases. Hence, the third and most important limitation of the above digraph algorithm is that it works only for kinetic schemes having corresponding path divergent trees with only one repeat node or ones with more than one repeat node appearing in the *same* stage or tier.

An example of a kinetic scheme yielding path divergent trees with multiple repeat nodes appearing in different stages or tiers is shown in Scheme 4, which is a more complete representation of the racemization process suggested by Scheme 2. Clearly, racemization between S_R and S_S necessarily takes place via a lower symmetry intermediate that is in equilibrium with both S_R and S_S since loss of chirality takes place via a bond-breaking process.

The corresponding path divergent trees are shown in Figs. 5*A* and 5*B*. Note that in Fig. 5*A* there is a repeat node

Fig. 5. Path divergent trees for paths emanating from SR (A) and SS (B). See Scheme 4.
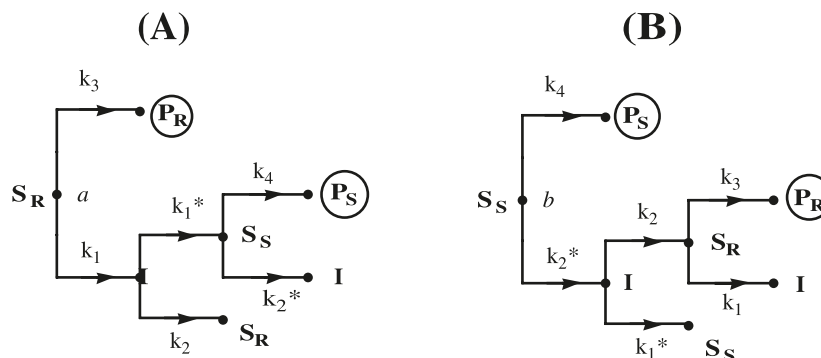
S_R that appears in the second tier and another repeat node I that appears in the third tier. Similarly, repeat nodes in different tiers are observed in Fig. 5B. Application of the above digraph algorithm leads to the incorrect expression for the final product ratio shown in eq. [14],

$$[14] \quad \frac{[P_R]_\infty}{[P_S]_\infty} = \left(\frac{k_3}{k_4}\right)\left[\frac{(a+b)\,k_2 k_2^* + ak_4(k_2 + k_1^*) + ak_1 k_1^*}{(a+b)\,k_1 k_1^* + bk_3(k_1 + k_2^*) + bk_2 k_2^*}\right]$$

The correct expression found by the Laplace transform method is shown in eq. [15],

$$[15] \quad \frac{[P_R]_\infty}{[P_S]_\infty} = \left(\frac{k_3}{k_4}\right)\left[\frac{(a+b)\,k_2 k_2^* + ak_4(k_2 + k_1^*)}{(a+b)\,k_1 k_1^* + bk_3(k_1 + k_2^*)}\right]$$

Note the extra terms appearing in the numerator and denominator in eq. [14]. The ACH limit applied to eq. [14] leads to eq. [16],

$$[16] \quad \left(\frac{[P_R]_\infty}{[P_S]_\infty}\right)_{ACH} = \left(\frac{k_3}{k_4}\right)\left[\frac{2a+b}{a+2b}\right]$$

which shows a dependency on the starting amounts of S_R and S_S, a and b. When this limit is applied to eq. [15], however, the result is the expected no dependence on a and b as shown by eq. [17],

$$[17] \quad \left(\frac{[P_R]_\infty}{[P_S]_\infty}\right)_{ACH} = \frac{k_3}{k_4}$$

A second digraph method based on a variation of the Chou algorithm is found to work for all cases and thus circumvents the third limitation of the above path divergent tree method, as will be shown next. Again using the same kinetic schemes shown in Schemes 1 and 2, the Chou digraph is constructed as shown Scheme 5.

The digraph is similar to that shown in Scheme 3 except that the rate constants connecting the nodes are assigned a negative sign and loops are added to those nodes that have kinetic arrows emanating from them. The rate-constant weights assigned to the loop nodes correspond to the positive sum of the rate constants emanating from them. From this digraph, all subgraphs are enumerated according to the following steps. For a given target product node, draw all paths that lead to it from all starting substrate nodes. All other points not traversed by this path are connected by cy-
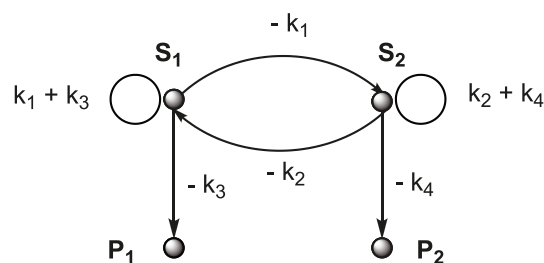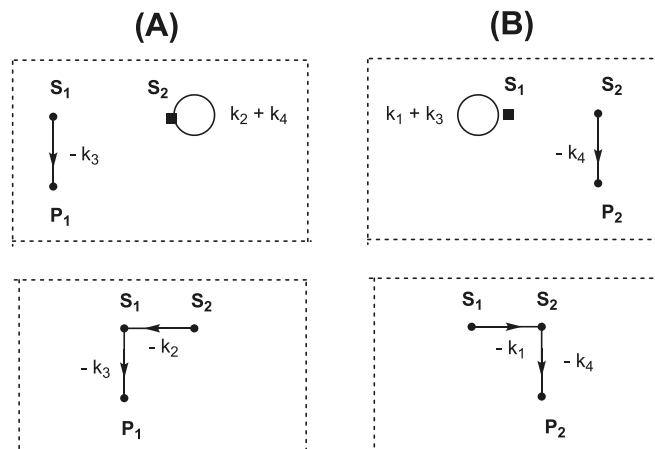
Scheme 5.

Fig. 6. Subgraphs from digraph shown in Scheme 5: (A) target product P_1; (B) target product P_2.


cles that neither intersect each other nor intersect the path. Repeat the process for all other target product nodes. The contributing expression to each target product node is given by eq. [18],

$$[18] \quad P_x \rightarrow \sum_{subgraph} \left[s_y(-1)^{n+c+1}\left(\prod_j k_j\right)\right]$$

where for a given subgraph, s_y is the starting amount of a starting node, n is the total number of nodes in the subgraph, c is the number of cycles, the product of rate-constant factors corresponds to all arrow and loop contributions, and the sum is taken over the number of subgraphs leading to common product node P_x. Hence, the subgraphs pertaining to the digraph in Scheme 5 are shown in Fig. 6.

Fig. 7. Digraph and subgraphs pertaining to Scheme 4.

Target Product: P_R Target Product: P_S

Fig. 8. Example acyclic equilibrium systems.
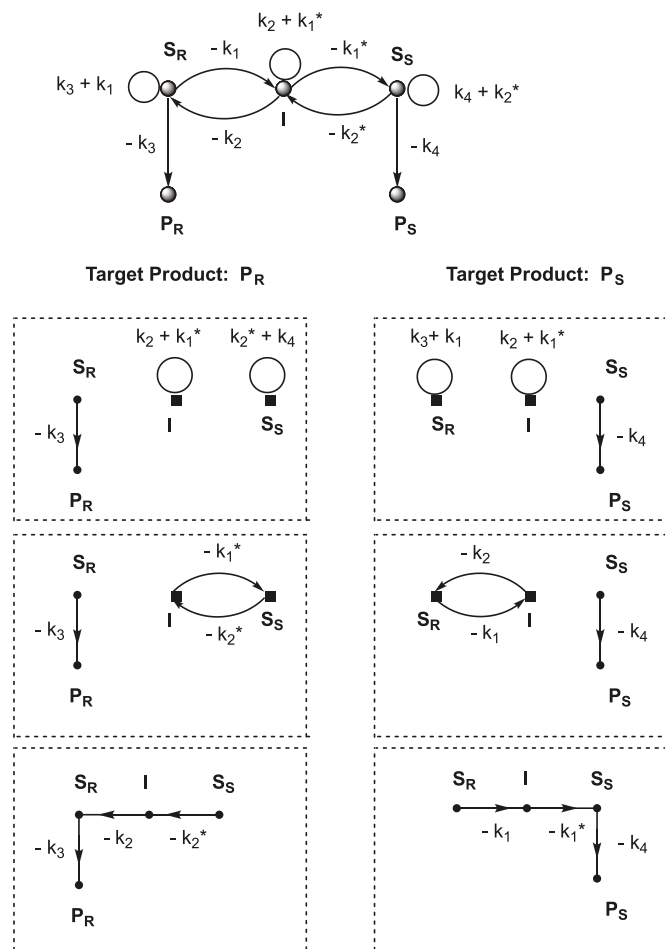
The contributing expression for the P_1 node is,

[19] $[P_1]_\infty \to a(-1)^{3+1+1}(-k_3)(k_2 + k_4)$

$+ b(-1)^{3+0+1}(-k_2)(-k_3) = k_3[(a + b)k_2 + k_4]$
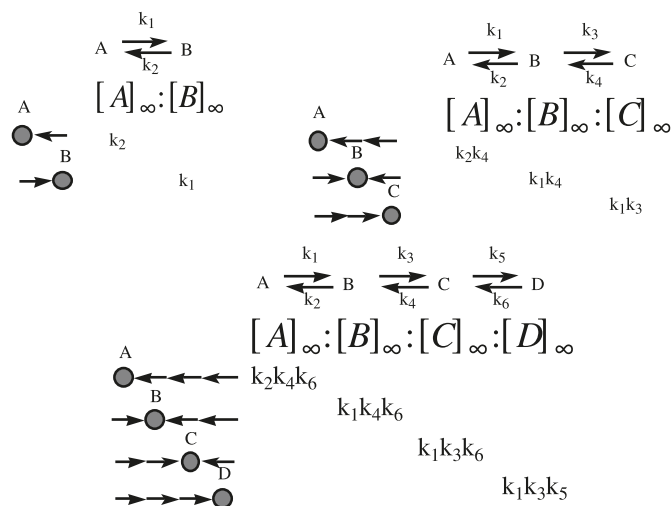
and that for the P_2 node is,

[20] $[P_2]_\infty \to b(-1)^{3+1+1}(-k_4)(k_1 + k_3)$

$+ a(-1)^{3+0+1}(-k_1)(-k_4) = k_4[(a + b)k_1 + k_3]$

Note the following transposition of variables: $a \leftrightarrow b$, $k_1 \leftrightarrow k_2$, $k_3 \leftrightarrow k_4$. Hence, the final product ratio is found by dividing eq. [19] by eq. [20], which leads immediately to the previous expression given in eq. [11] found by the first digraph method based on path divergent trees. The application of the adapted Chou method to the kinetic scheme shown in Scheme 4 yields the digraph and subgraphs shown in Fig. 7.

The resulting contributing expressions for P_R and P_S are given by eqs. [21] and [22],

[21] $[P_R]_\infty \to a[(-1)^{4+2+1}(-k_3)(k_2 + k_1^*)(k_2^* + k_4)$

$+ (-1)^{4+1+1}(-k_3 k_1^* k_2^*)] + b(-1)^{4+0+1}(-k_2^* k_2 k_3)$

$= ak_3(k_2 k_2^* + k_2 k_4 + k_1^* k_4) + bk_2 k_2^* k_3$

[22] $[P_S]_\infty \to b[(-1)^{4+2+1}(-k_4)(k_1 + k_2^*)(k_1^* + k_3)$

$+ (-1)^{4+1+1}(-k_4 k_2^* k_1^*)] + a(-1)^{4+0+1}(-k_1^* k_1 k_4)$

$= bk_4(k_1 k_1^* + k_1 k_3 + k_2^* k_3) + ak_1 k_1^* k_4$

The ratio of these expressions is in agreement with the expected result given by eq. [15].

It is clear that the present new digraph methods confer key advantages that can be used to tackle rather complex schemes leading to multiple products that would otherwise be daunting to analyze by conventional means as will be shown, vide infra.

Equilibrium systems

The basic idea of keeping track of the arrow directionality in kinetic schemes may be used to full advantage to determine final equilibrium ratios of chemical species connected only by reversible steps by inspection, with almost no work involved. Figure 8 shows the results for acyclic equilibrium systems involving two, three, and four species in a linear arrangement. One can observe key patterns among these examples. If there are N species in an acyclic equilibrium, each term of the product ratio consists of N – 1 rate constants. The final equilibrium concentration expression for each species is determined by a single term equal to a product of rate constants corresponding to the combination of reaction arrows that points towards that species. For example, for the case of four species in an acyclic arrangement, the term for the final concentration of species A consists of a single product of three rate constants with descriptors 2, 4, and 6, which correspond to those that point toward A.

For cyclic equilibrium systems, the situation is more complicated but still can be deduced by the simple technique of following the reaction arrow directionality. Figure 9 shows the results for cyclic equilibrium systems involving three and four species. If there are N species in a cyclic equilibrium, each equilibrium product concentration expression consists of a sum of N terms, each of which consists of a product of N – 1 rate constants. The arrow directionality falls between the limiting clockwise and counter-clockwise

Fig. 9. Example cyclic equilibrium systems.
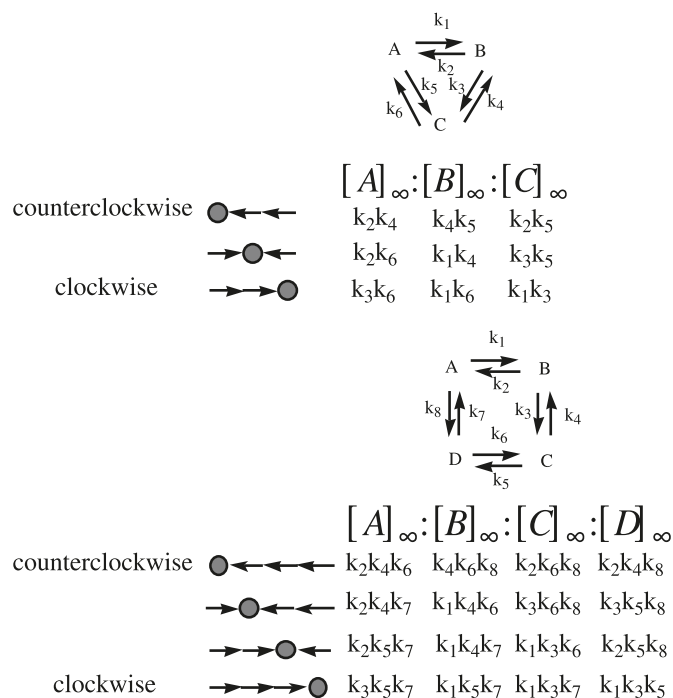
Scheme 6.

Scheme 7.

senses. For example, for the case of three species in a cyclic arrangement, the term for the final concentration of species A consists of a sum of three terms, each of which is composed of a product of two rate constants with pairwise descriptors (2,4), (2,6), and (3,6).

Extended variants of ACH kinetic schemes

In this section we examine extended variants of Scheme 1 in acyclic and cyclic arrangements and determine their associated initial and final product ratio expressions by the adapted Chou directed graph method. Consider the linear and cyclic triads shown in Schemes 6 and 7 with initial conditions $[A]_0 = a$, $[B]_0 = b$, and $[C]_0 = c$.
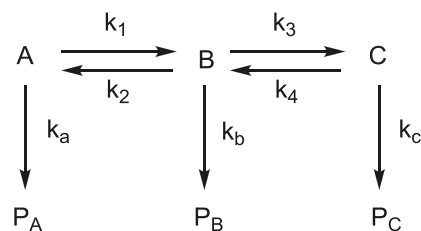
The determination of the final product ratios as given in the Supplementary Data results in the following relationships for the linear and cyclic triads, respectively,[2]

[23] $[P_A]_\infty:[P_B]_\infty:[P_C]_\infty$

$$= k_A\{a[(k_A + k_2)(k_4 + k_C) + k_3k_C] + bk_2(k_4 + k_C) + ck_2k_4\}$$
$$: k_B\{ak_1(k_4 + k_C) + b(k_A + k_1)(k_4 + k_C) + ck_4(k_A + k_1)\}$$
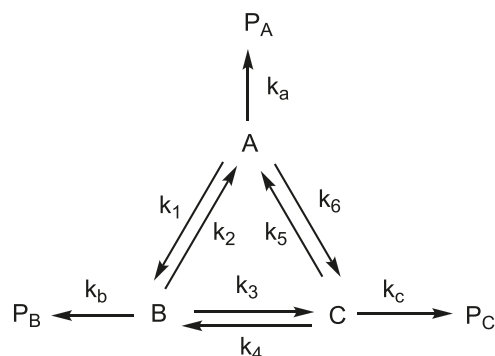$$: k_C\{ak_1k_3 + bk_3(k_A + k_1) + c[(k_A + k_1)(k_3 + k_C) + k_2k_A]\}$$

[24] $[P_A]_\infty:[P_B]_\infty:[P_C]_\infty$

$$= k_A\{a[(k_B + k_2)(k_4 + k_5 + k_C) + k_3(k_C + k_5)] + b[k_2(k_4 + k_5 + k_C) + k_3k_5] + c[k_5(k_2 + k_3 + k_B)k_2k_4]\}$$
$$: k_B\{a[k_1(k_4 + k_5 + k_C) + k_4k_6] + b[(k_A + k_1)(k_4 + k_5 + k_C) + k_6(k_C + k_4)] + c[k_4(k_A + k_1 + k_6)k_1k_5]\}$$
$$: k_C\{a[k_6(k_2 + k_3 + k_B) + k_1k_3] + b[k_3(k_A + k_1 + k_6) + k_2k_6] + c[(k_A + k_6)(k_2 + k_3 + k_B) + k_1(k_B + k_3)]\}$$

In both cases the initial product ratio based on the shortest paths from A, B, and C to the respective target products is $[P_A]_0:[P_B]_0:[P_C]_0 = ak_A:bk_B:ck_C$. Also, in both cases the ACH limit and the anti-ACH limit lead to final product ratios of $([P_A]_\infty:[P_B]_\infty:[P_C]_\infty)_{ACH} = k_A:k_B:k_C$ and $([P_A]_\infty:[P_B]_\infty: [P_C]_\infty)_{anti-ACH} = a:b:c$, respectively. These re-

sults may be extended to tetrad, pentad, etc. arrangements of chemical species in equilibrium, each producing a unique product in an irreversible product-forming step. We may conclude that the forms of final product ratio expressions for both ACH anti-ACH limiting conditions are universal.

Generalization of kinetic plasticity in DKR systems

As demonstrated for Scheme 3, the key plot needed to determine the degree of kinetic plasticity is that given in Fig. 1, in which the final product excess is plotted against the initial substrate excess. The implication is that kinetic plasticity is defined in a pairwise sense since pairwise comparisons are made between pairs of products and pairs of substrates. For the trivial case of Scheme 3, there is only one pair of products and one pair of substrates. By analogy with the previous analysis based on limiting slopes, we may generalize the expression for kinetic plasticity starting from inequality [25],

[25] $\text{slope}_{ACH} < \text{slope}_{exp} < \text{slope}_{anti\text{-}ACH}$

Subtracting slope_{ACH} from all terms results in

[26] $0 < \text{slope}_{exp} - \text{slope}_{ACH} < \text{slope}_{anti\text{-}ACH}$
$$- \text{slope}_{ACH}$$

Dividing all terms by $(\text{slope}_{anti\text{-}ACH} - \text{slope}_{ACH})$ results in

[27] $0 < \dfrac{\text{slope}_{exp} - \text{slope}_{ACH}}{\text{slope}_{anti\text{-}ACH} - \text{slope}_{ACH}} < 1$

Using this definition, we may revise the ACH principle simply by stating that a kinetic model in which products are formed from equilibrating substrates satisfies the ACH condition when its degree of plasticity is 100%. For the kinetic model in Scheme 3, $\text{slope}_{ACH} = 0$ and $\text{slope}_{anti\text{-}ACH} = 1$, which implies by inequality [27] that $0 < \text{slope}_{exp} < 1$ is satisfied. The kinetic plasticity in this case was defined as $\varepsilon_{DKR} = 1 - \text{slope}_{exp}$ to make the zero value and the unit value in inequality [27] correspond to 100% plasticity and 0% plasticity, respectively. Hence for Scheme 3, eq. [8] resulted. Maintaining this sense, the general expression for kinetic plasticity becomes,

[28] $\varepsilon_{DKR} = 1 - \dfrac{\text{slope}_{exp} - \text{slope}_{ACH}}{\text{slope}_{anti\text{-}ACH} - \text{slope}_{ACH}} = 1 - \text{slope}_{exp}$

The determination of kinetic plasticity parameters for any kinetic scheme, such as those shown in Schemes 6 and 7, must be done on a pairwise basis such that adjacent pairs of products arising from their corresponding equilibrating substrates are considered. For example, for Scheme 6 there are three substrates leading to three unique products, and there are two pairs of adjacent products to consider in the pairwise analysis. This will result in two kinetic plasticity indices corresponding to the $P_A P_B$ and $P_B P_C$ pairs of products. The global kinetic plasticity for the scheme would be described by this set of two indices. The form of the expression for the kinetic plasticity index would be identical to eq. [8] with $r = k_a/k_b$, $u = k_1/k_a$, and $v = k_2/k_a$ for the $P_A P_B$ pair, and $r = k_b/k_c$, $u = k_3/k_b$, and $v = k_4/k_b$ for the $P_B P_C$ pair. For Scheme 7 there are three adjacent pairs of products to consider, leading to three kinetic plasticity parameters: $P_A P_B$, $P_B P_C$, and $P_A P_C$. Again, eq. [8] applies with $r = k_a/k_b$, $u = k_1/k_a$, and $v = k_2/k_a$ for the $P_A P_B$ pair; $r = k_b/k_c$, $u = k_3/k_b$, and $v = k_4/k_b$ for the $P_B P_C$ pair; and $r = k_a/k_c$, $u = k_6/k_a$, and $v = k_5/k_a$ for the $P_A P_C$

pair. Unfortunately for both Schemes 6 and 7, it is not possible to obtain the kinetic plasticity indices directly by conducting product study experiments by varying in a pairwise fashion the initial substrate ratio as a function of the corresponding final product ratio, since neat expressions of the form of eq. [5] are not obtainable. Instead, the magnitudes of all rate constants need to be determined directly by independent kinetic experiments to make estimates of the above pairs of kinetic plasticity parameters using eq. [8].

Dynamic kinetic resolution by organocatalysis

The emerging field of organocatalysis (65–86) has undergone a rapid growth in recent years and provides several opportunities to test ideas presented in this work. Three examples are presented in which the versatility of the directed graph methods is applied to determine initial and final product ratio expressions. Corresponding expressions for the kinetic plasticity index are also determined in each case. These examples showcase the prowess of the new methods in tackling complex schemes with apparent ease. In addition, the new suggested product study experiment and corresponding linear relationship according to eq. [5] serves as a diagnostic test to verify the proposed kinetic schemes for these chemical systems and offers an opportunity to properly quantify their kinetic plasticities directly from experiment.

The first example (87) shown in Scheme 8 involves a double feed-in reaction that first produces racemizable chiral imine intermediates from chiral aldehydes and aromatic amines, followed by catalytic production of chiral iminium salts that are then finally reduced to their amine analogues via oxidation of Hantzsch dihydropyridine esters to pyridines. Figure 10 shows the corresponding directed graph and Section 6 of the Supplementary Data shows the list of subgraphs to consider with respect to P_1 as the target product by the adapted Chou method.[2] The subgraphs with respect to P_2 as the target product are found using the following transposition of variables: $[A]_0 \leftrightarrow [B]_0$, $k_1 \leftrightarrow k_8$, $k_2 \leftrightarrow k_7$, $k_3 \leftrightarrow k_6$, $k_4 \leftrightarrow k_5$, $k_9 \leftrightarrow k_{10}$, and $k_{11} \leftrightarrow k_{12}$. For the analysis it was assumed that the concentrations of aromatic amine, chiral acids HX*, and Hanzsch dihydropyridine esters were in excess compared with the chiral aldehydes A and B. The expressions for the initial and final product ratios and the final product excess are given by eqs. [29], [30], and [31],

[29] $\dfrac{[P_1]_0}{[P_2]_0} = \dfrac{[A]_0}{[B]_0}\left(\dfrac{k_1}{k_8}\right)\left(\dfrac{k_9 k_{11}}{k_{10} k_{12}}\right)$

[30] $\dfrac{[P_1]_\infty}{[P_2]_\infty} = \left(\dfrac{k_9}{k_{10}}\right)\left[\dfrac{[A]_0\alpha + [B]_0 k_4 k_6}{[A]_0 k_3 k_5 + [B]_0\beta}\right]$

where

$\alpha = k_4 k_6 + k_{10}[HX^*](k_4 + k_5)$
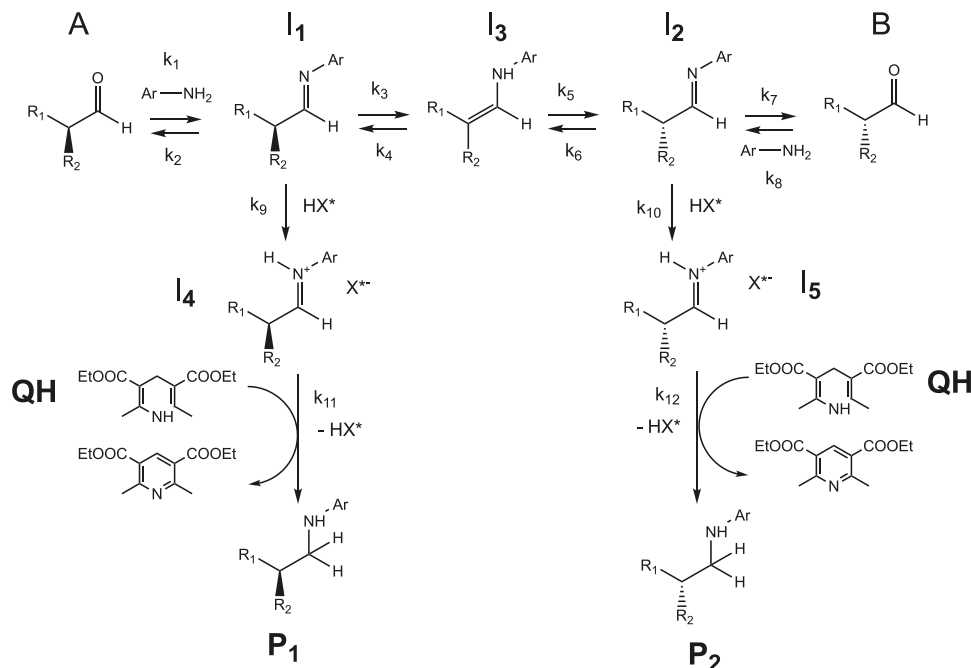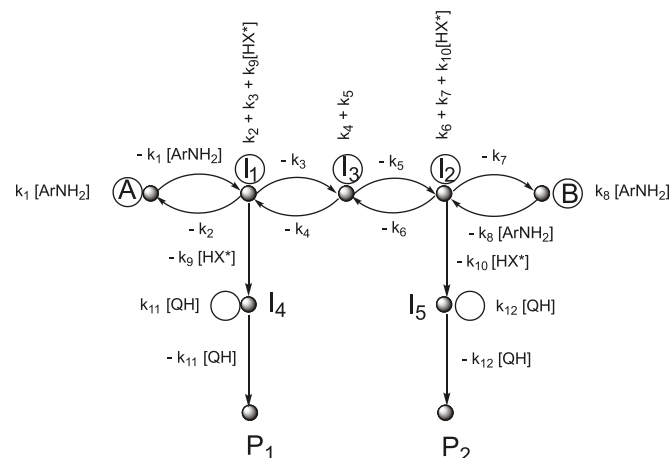
$\beta = k_3 k_5 + k_9[HX^*](k_4 + k_5)$

Scheme 8.

Fig. 10. Chou digraph pertaining to Scheme 8.

$$[32] \quad \alpha = k^2 + k_{10}[\text{HX}^*]2k$$

$$\beta = k^2 + k_9[\text{HX}^*]2k$$

so that the final product ratio becomes,

$$[33] \quad \left(\frac{[\text{P}_1]_\infty}{[\text{P}_2]_\infty}\right)_{\text{ACH}}$$

$$= \lim_{k\to\infty}\left(\frac{k_9}{k_{10}}\right)\left[\frac{[\text{A}]_0(k^2 + k_{10}[\text{HX}^*]2k) + [\text{B}]_0 k^2}{[\text{A}]_0 k^2 + [\text{B}]_0(k^2 + k_9[\text{HX}^*]2k)}\right]$$

$$= \left(\frac{k_9}{k_{10}}\right)\lim_{k\to\infty}\left[\frac{([\text{A}]_0 + [\text{B}]_0)k^2 + [\text{A}]_0(k_{10}[\text{HX}^*]2k)}{([\text{A}]_0 + [\text{B}]_0)k^2 + [\text{B}]_0(k_9[\text{HX}^*]2k)}\right]$$

$$= \left(\frac{k_9}{k_{10}}\right)\left(\frac{[\text{A}]_0 + [\text{B}]_0}{[\text{A}]_0 + [\text{B}]_0}\right)$$

$$= \frac{k_9}{k_{10}}$$

which shows a dependence only on the product forming rate constants emanating from intermediates I1 and I2.

In the anti-ACH limit when $k_i = k$ (for $i = 1$ to 8) and are very small compared with k_j (for $j = 9$ to 12), we have the same relations as in eq. [32] so that the final product ratio becomes,

$$[34] \quad \left(\frac{[\text{P}_1]_\infty}{[\text{P}_2]_\infty}\right)_{\text{anti-ACH}}$$

$$= \lim_{k\to 0}\left(\frac{k_9}{k_{10}}\right)\left[\frac{[\text{A}]_0(k^2 + k_{10}[\text{HX}^*]2k) + [\text{B}]_0 k^2}{[\text{A}]_0 k^2 + [\text{B}]_0(k^2 + k_9[\text{HX}^*]2k)}\right]$$

$$[31] \quad pe_\infty = \frac{\left(\dfrac{k_9}{k_{10}}\right)\left(\dfrac{[\text{A}]_0\alpha + [\text{B}]_0 k_4 k_6}{[\text{A}]_0 k_3 k_5 + [\text{B}]_0\beta}\right) - 1}{\left(\dfrac{k_9}{k_{10}}\right)\left(\dfrac{[\text{A}]_0\alpha + [\text{B}]_0 k_4 k_6}{[\text{A}]_0 k_3 k_5 + [\text{B}]_0\beta}\right) + 1}$$

$$= \frac{ru_2 v_1 - u_1 v_2}{ru_2 v_1 + u_1 v_2 + [\text{HX}^*](v_1 + v_2)}$$

$$+ \left(\frac{[\text{A}]_0 - [\text{B}]_0}{[\text{A}]_0 + [\text{B}]_0}\right)\left(\frac{[\text{HX}^*](v_1 + v_2)}{ru_2 v_1 + u_1 v_2 + [\text{HX}^*](v_1 + v_2)}\right)$$

where $r = k_9/k_{10}$, $u_1 = k_3/k_{10}$, $u_2 = k_6/k_{10}$, $v_1 = k_4/k_{10}$, and $v_2 = k_5/k_{10}$. Note that eq. [31] shows a linear dependence between pe_∞ and se_0. In the ACH limit when $k_i = k$ (for $i = 1$ to 8) and are very large compared with k_j (for $j = 9$ to 12), we have,

Scheme 9.
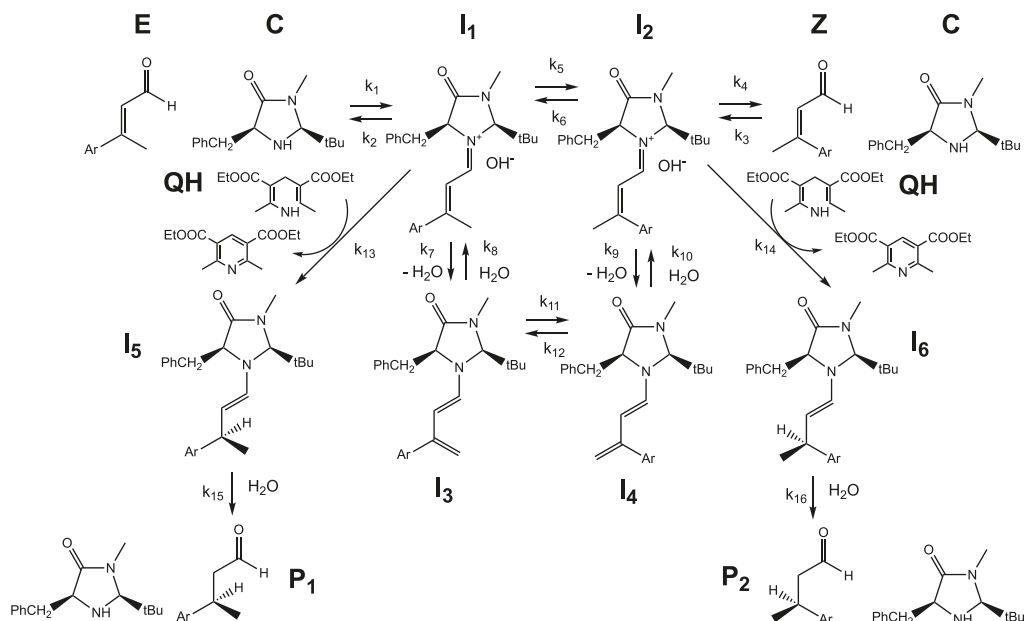
$$= \left(\frac{k_9}{k_{10}}\right) \lim_{k \to 0} \left[\frac{([A]_0 + [B]_0)k^2 + [A]_0(k_{10}[HX^*]2k)}{([A]_0 + [B]_0)k^2 + [B]_0(k_9[HX^*]2k)} \right]$$

$$= \left(\frac{k_9}{k_{10}}\right)\left(\frac{[A]_0}{[B]_0}\right)\left(\frac{k_{10}}{k_9}\right)\left(\frac{2[HX^*]}{2[HX^*]}\right)$$

$$= \frac{[A]_0}{[B]_0}$$

which shows a dependence only on the starting amounts of aldehydes A and B.

The final product excess as a function of initial substrate excess for these two limits is given by eqs. [35] and [36],

$$[35] \quad (\text{pe}_\infty)_{\text{ACH}} = \lim_{\substack{u_i \to \infty \\ v_i \to \infty}} \text{pe}_\infty = \frac{r-1}{r+1} = \frac{\dfrac{k_9}{k_{10}} - 1}{\dfrac{k_9}{k_{10}} + 1}$$

$$[36] \quad (\text{pe}_\infty)_{\text{anti-ACH}} = \lim_{\substack{u_i \to \infty \\ v_i \to \infty}} \text{pe}_\infty = \text{se}_0$$

where

$$\text{se}_0 = \frac{[A]_0 - [B]_0}{[A]_0 + [B]_0}$$

Using the definition given in eq. [28], the expression for the kinetic plasticity for this kinetic model is given by eq. [37],

$$[37] \quad \varepsilon_{\text{DKR}} = 1 - \frac{\left(\dfrac{d(\text{pe}_\infty)}{d(\text{se}_0)}\right)_{\text{exp}} - \left(\dfrac{d(\text{pe}_\infty)}{d(\text{se}_0)}\right)_{\text{ACH}}}{\left(\dfrac{d(\text{pe}_\infty)}{d(\text{se}_0)}\right)_{\text{anti-ACH}} - \left(\dfrac{d(\text{pe}_\infty)}{d(\text{se}_0)}\right)_{\text{ACH}}}$$

$$\left(\dfrac{d(\text{pe}_\infty)}{d(\text{se}_0)}\right)_{\text{exp}} - 0$$
$$= 1 - \frac{}{1 - 0}$$

$$= 1 - \left(\frac{d(\text{pe}_\infty)}{d(\text{se}_0)}\right)_{\text{exp}}$$

$$= 1 - \frac{[HX^*](v_1 + v_2)}{ru_2v_1 + u_1v_2 + [HX^*](v_1 + v_2)}$$

$$= \frac{ru_2v_1 + u_1v_2}{ru_2v_1 + u_1v_2 + [HX^*](v_1 + v_2)}$$

The second example (88) shown in Scheme 9 is a more complex variant of Scheme 8. The aim is to stereoselectively reduce a mixture of (E/Z) α,β-unsaturated aldehydes to their dihydroaldehyde analogs via Hanzsch dihydropyridines and a chiral organocatalyst that produces (E/Z) iminium intermediates that are interconvertible. Figure 11 shows the corresponding directed graph and Section 7 of the Supplemenatry Data shows the subgraphs with respect to P1 as the target product.[2] As in the previous case, the subgraphs with respect to P_2 are found using the following transposition of variables: $[E]_0 \leftrightarrow [Z]_0$, $k_1' \leftrightarrow k_3'$, $k_2 \leftrightarrow k_4$, $k_5 \leftrightarrow k_6$, $k_7 \leftrightarrow k_9$, $k_8' \leftrightarrow k_{10}'$, $k_{11} \leftrightarrow k_{12}$, $k_{13}' \leftrightarrow k_{14}'$, and $k_{15}' \leftrightarrow k_{16}'$.
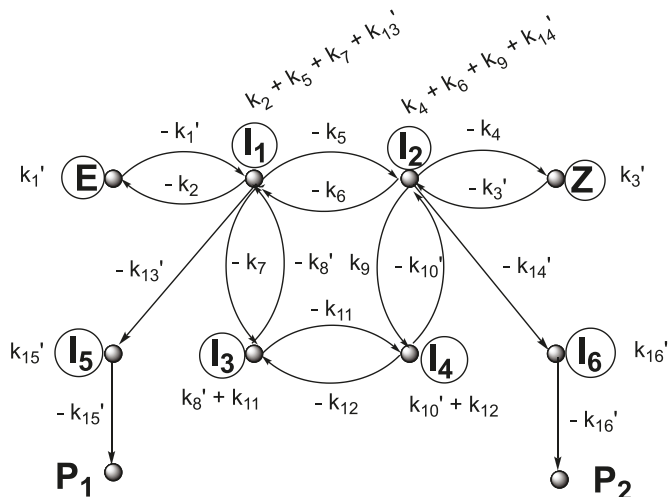
The expressions for the initial and final product ratios and the final product excess are given by eqs. [38], [39], and [40],

$$[38] \quad \frac{[P_1]_0}{[P_2]_0} = \frac{[E]_0}{[Z]_0}\left(\frac{k_1}{k_3}\right)\left(\frac{k_{13}k_{15}}{k_{14}k_{16}}\right)$$

$$[39] \quad \frac{[P_1]_\infty}{[P_2]_\infty} = \left(\frac{k_{13}'}{k_{14}'}\right)\left(\frac{([E]_0 + [Z]_0)\alpha + [E]_0 k_{14}'\beta}{([E]_0 + [Z]_0)\alpha^* + [E]_0 k_{13}'\beta}\right)$$

where

Fig. 11. Chou digraph pertaining to Scheme 9.

$$\alpha = k_6\beta + k_9 k'_8 k_{12}$$

$$\alpha^* = k_5\beta + k_7 k'_{10} k_{11}$$

$$\beta = k'_8 k'_{10} + k'_8 k'_{12} + k'_{10} k'_{11}$$

$$k'_1 = k_1[C], \quad k'_3 = k_3[C], \quad k'_8 = k_8[H_2O],$$

$$k'_{10} = k_{10}[H_2O]$$

$$k'_{15} = k_{15}[H_2O], \quad k'_{16} = k_{16}[H_2O],$$

$$k'_{13} = k_{13}[QH], \quad k'_{14} = k_{14}[QH]$$

$$[40] \quad pe_\infty = \frac{\left(\dfrac{k'_{13}}{k'_{14}}\right)\left[\dfrac{([E]_0 + [Z]_0)\alpha + [E]_0 k'_{14}\beta}{([E]_0 + [Z]_0)\alpha^* + [E]_0 k'_{13}\beta}\right] - 1}{\left(\dfrac{k'_{13}}{k'_{14}}\right)\left[\dfrac{([E]_0 + [Z]_0)\alpha + [E]_0 k'_{14}\beta}{([E]_0 + [Z]_0)\alpha^* + [E]_0 k'_{13}\beta}\right] + 1}$$

$$= \frac{r\alpha - \alpha^*}{r\alpha + \alpha^* + k'_{13}\beta} + \left(\frac{[E]_0 - [Z]_0}{[E]_0 + [Z]_0}\right)\left(\frac{k'_{13}\beta}{r\alpha + \alpha^* + k'_{13}\beta}\right)$$

where $r = k'_{13}/k'_{14}$. Note that eq. [40] shows a linear dependence between pe_∞ and se_0. In the ACH limit when $k_i = k$ (for $i = 1$ to 12) and very large compared with k_j (for $j = 13$ to 16), we have

$$\alpha \to 4k^3$$

$$[41] \quad \alpha^* \to 4k^3$$

$$\beta \to 3k^2$$

so that the final product ratio becomes,

$$[42] \quad \left(\frac{[P_1]_\infty}{[P_2]_\infty}\right)_{ACH}$$

$$= \lim_{k \to \infty} \left(\frac{k'_{13}}{k'_{14}}\right)\left[\frac{([E]_0 + [Z]_0)4k^3 + [E]_0 k'_{14}3k^2}{([E]_0 + [Z]_0)4k^3 + [Z]_0 k'_{13}3k^2}\right]\left(\frac{k'_{13}}{k'_{14}}\right)$$

which shows, as in the previous example, a dependence only on the ratio of product forming rate constants emanating from intermediates I_1 and I_2.

In the anti-ACH limit when $k_i \longrightarrow 0$ (for $i = 1$ to 12), we have the same relations as in eq. [41], so that the final product ratio becomes,

$$[43] \quad \left(\frac{[P_1]_\infty}{[P_2]_\infty}\right)_{anti-ACH}$$

$$= \lim_{k \to 0} \left(\frac{k'_{13}}{k'_{14}}\right)\left[\frac{([E]_0 + [Z]_0)4k^3 + [E]_0 k'_{14}3k^2}{([E]_0 + [Z]_0)4k^3 + [Z]_0 k'_{13}3k^2}\right]\left(\frac{[E]_0}{[Z]_0}\right)$$

The final product excess as a function of initial substrate excess for these two limits are given by eqs. [44] and [45],

$$[44] \quad (pe_\infty)_{ACH} = \frac{r - 1}{r + 1} = \frac{\dfrac{k'_{13}}{k'_{14}} - 1}{\dfrac{k'_{13}}{k'_{14}} + 1}$$

$$[45] \quad (pe_\infty)_{anti-ACH} = se_0$$

where

$$se_0 = \frac{[A]_0 - [B]_0}{[A]_0 + [B]_0}$$

Using the definition given in eq. [28], the expression for the kinetic plasticity for this kinetic model is given by eq. [46],

$$[46] \quad \varepsilon_{DKR} = \frac{r\alpha + \alpha^*}{r\alpha + \alpha^* + k'_{13}\beta}$$

The final example (89) shown in Scheme 10 involves stereoselective α-fluorination via an electrophilic "F⁺" species of an achiral aldehyde using a chiral proline analogue as an organocatalyst. The two products of interest are P_1 and P_2. The third difluorinated product arises from intermediate I_4 which is in equilibrium with I_2 and I_3. All three products arise from the same source, namely intermediate I_1. Since the products do not arise from different equilibrating starting substrates, kinetic control to produce one of the products over the others will depend on the relative magnitudes of the rate constants and not on the initial amount of starting material. Figure 12 shows the corresponding directed graph and Section 8 of the Supplementary Data shows the subgraphs with respect to P_1, P_2, and P_3 as the target products.[2] The following transposition of variables applies: $k'_3 \leftrightarrow k'_8$, $k_7 \leftrightarrow k_9$, $k'_5 \leftrightarrow k'_8$, and $k'_8 \leftrightarrow k'_{10}$. The initial and final product ratios are given by eqs. [47] and [48], respectively.

$$[47] \quad [P_1]_0:[P_2]_0:[P_3]_0 = k'_3 k'_5 : k'_4 k'_6 : k'_{11} k'_{12}(k'_3 k_7 + k'_4 k_9)$$

$$[48] \quad [P_1]_\infty:[P_2]_\infty:[P_3]_\infty$$

$$= k'_5\{k'_3 k'_6 \alpha + k_9(k'_3 k'_8 + k'_4 k'_8 + k'_3 k'_{11})\}$$

$$: k'_6\{k'_4 k'_5 \alpha + k_7(k'_4 k'_{10} + k'_4 k'_{11} + k'_3 k'_{10})\}$$

$$: k'_{11}\{k'_3 k_7(k'_6 + k_9) + k'_4 k_9(k'_5 + k_7)\}$$

where

© 2008 NRC Canada

Scheme 10.

$\alpha = k'_8 + k'_{10} + k'_{11}$

$k_3' = k_3[F^+], \ k_4' = k_4[F^+], \ k'_{11} = k_{11}[F^+]$

$k'_5 = k_5[H_2O], \ k'_6 = k_6[H_2O], \ k'_8 = k_8[H_2O]$

$k'_{10} = k_{10}[H_2O], \ k'_{12} = k_{12}[H_2O]$

In the ACH limit when there is rapid equilibration between intermediates I_2, I_3, and I_4 so that $k_i = k$ (for $i = 7$ to 10) is very large compared with the product forming rate constants, then the final product ratio becomes,

[49] $([P_1]_\infty:[P_2]_\infty:[P_3]_\infty)_{ACH}$

$= k'_5:k'_6:k'_{11} = k_5[H_2O]:k_6[H_2O]:k_{11}[F^+]$

Again, these are the product-forming rate constants emanating from intermediates I_2, I_3, and I_4. On the other hand, the anti-ACH limit results in a final product ratio given by eq. [50], which predicts the absence of the difluorinated product P_3,

[50] $([P_1]_\infty:[P_2]_\infty:[P_3]_\infty)_{anti\text{-}ACH} = k'_3:k'_4:0$

Since all three products arise from the same source substrate, it is not possible to obtain estimates of kinetic plasticity parameters for this scheme by varying substrate amounts. Direct estimates of the appropriate rate constants need to be made. The two pairs of products to consider are P_1P_3 and P_3P_2 that will lead to two kinetic plasticity indices. They will be of the form of eq. [8] with $r = k'_5/k'_{11}$, $u = k_7/k'_5$, and $v = k'_8/k'_5$ for the P_1P_3 pair and $r = k'_{11}/k'_6$, $u = k'_{10}/k'_{11}$, and $v = k_9/k'_{11}$ for the P_3P_2 pair.

Fig. 12. Chou digraph pertaining to Scheme 10.

Conclusions

The present work introduces new algorithms based on directed graphs to determine initial and final product ratios for simple and complex kinetic models leading to multiple products for unimolecular transformations and under pseudo-order conditions. These are found to circumvent the tedious and error prone computations that are characteristic of conventional treatments based on rate laws. A degree of kinetic plasticity parameter is introduced and shown to be general in

describing the ACH condition (100% dynamic kinetic resolution), the opposite anti-ACH condition (0% dynamic kinetic resolution), and all other scenarios in between these limits. To empirically probe the full scope of the dynamics of a kinetic system one needs to begin from more than one set of starting substrate conditions. Thus, it is impossible to obtain a full picture by carrying out product studies from one set of starting substrate conditions such as a racemic mixture. For a practicing organic chemist who wishes to understand their kinetic schemes more deeply without having to invoke external assumptions, this means that they must move beyond the confines of racemic mixtures as the only starting point to obtain direct experimental measures of the dynamics of their systems. The determination of the degree of kinetic plasticity is thus based on a key experimental plot that relates final product excess and initial substrate excess in a pairwise fashion. Such a plot is always linear with a positive slope, and the degree of kinetic plasticity is found directly by subtracting the slope from unity. Furthermore, it may be used as a diagnostic test for checking the validity of proposed ACH-type kinetic schemes for a given chemical system. A key bonus of the new methods of obtaining product ratio expressions is that the precise rate constant dependence of the degree of kinetic plasticity is obtained explicitly. Such dependencies may be further checked by direct determination of absolute rate constants from independent kinetic measurements. Examination of extended variants of ACH-type schemes indicates that the ACH principle holds universally and may be elevated to the status of a kinetic theorem. The next challenge for organic chemists is to provide experimental verification of the predictions made in this work.

Acknowledgements

References

1. D.Y. Curtin. Rec. Chem. Prog. **15**, 111 (1954).
2. L.P. Hammett. Physical organic chemistry: reaction rates, equilibria, and mechanisms. 2nd ed. McGraw-Hill, New York. 1970. pp. 119–120.
3. S.F. Acree. Am. Chem. J. **38**, 1 (1907).
4. S. Winstein and N.J. Holness. J. Am. Chem. Soc. **77**, 5562 (1955).
5. J. Andraos. Chemical educator. In press.
6. E.L. Eliel, S.H. Wilen, and L.N. Mander. Stereochemistry of organic compounds. Wiley, New York. YEAR. pp. 647–655.
7. F.A. Carroll. Perspectives in structure and mechanism in organic chemistry. Brooks Cole Publishing Co., New York. 1998. pp. 345–349.
8. F.A. Carey and R.J. Sundberg. Advanced organic chemistry. Part A: structure and mechanism. Plenum Publishing, New York. 1993. pp. 209–216.
9. (*a*) J.I. Seeman. Chem. Rev. **83**, 83 (1983); (*b*) J.I. Seeman and W.A. Farone. J. Org. Chem. **43**, 1854 (1978).
10. J.I. Seeman. J. Chem. Educ. **63**, 42 (1986).
11. J. Andraos. J. Phys. Chem. A, **107**, 2374 (2003).
12. B. Martin-Matute, J.E. Bäckvall. Curr. Opin. Chem. Biol. **11**, 226 (2007).
13. J.E. Bäckvall. *In* Asymmetric catalysis. *Edited by* M. Christmann and S. Braese. Wiley-VCH, Weinheim, Germany. 2007. pp. 171–175.
14. E. Fogassy, M. Nogradi, D. Kozma, G. Egri, E. Palovics, and V. Kiss. Org. Biomol. Chem. **4**, 3011 (2006).
15. U.T. Bornscheuer. Adv. Biochem. Eng. Biotechnol. **100**, 181 (2005).
16. N.J. Turner. Curr. Opin. Chem. Biol. **8**, 114 (2004).
17. O. Pamies and J.E. Bäckvall. Trends Biotechnol. **22**, 130 (2004).
18. H. Pellissier. Tetrahedron, **59**, 8291 (2003).
19. O. Pamies and J.E. Bäckvall. Curr. Opin. Biotechnol. **14**, 407 (2003).
20. N.J. Turner. Curr. Opin. Biotechnol. **14**, 401 (2003).
21. O. Pamies and J.E. Bäckvall. Chem. Rev. **103**, 3247 (2003).
22. B. Schnell, K. Faber, and W. Kroutil. Adv. Synth. Catal. **345**, 653 (2003).
23. D.E.J.E. Robinson and S.D. Bull. Tetrahedron: Asymmetry, **14**, 1407 (2003).
24. M.J. Kim, Y. Ahn, and J. Park. Curr. Opin. Biotechnol. **13**, 578 (2002).
25. J.M.J. Williams, R.J. Parker, and C. Neri. *In* Enzyme catalysis in organic synthesis. Vol. 1. *Edited by* K. Drauz and H. Waldmann. Wiley-VCH, Weinheim, Germany. 2002. pp. 287–312.
26. O. May, S. Verseck, A. Bommarius, and K. Drauz. Org. Process Res. Dev. **6**, 452 (2002).
27. F.F. Huerta, A.B.E. Minidis, and J.E. Bäckvall. Chem. Soc. Rev. **30**, 321 (2001).
28. K. Faber. Chem. Eur. J. **7**, 5005 (2001).
29. G.R. Cook. Curr. Org. Chem. **4**, 869 (2000).
30. U.T. Strauss, U. Felfer, and K. Faber. Tetrahedron: Asymmetry, **10**, 107 (1999).
31. R.S. Ward. Selectivity in organic synthesis. Wiley, New York. 1999. Chap. 6.
32. M.T. El Gihani, J.M.J. Williams. Curr. Opin. Chem. Biol. **3**, 11 (1999).
33. R.J. Parker and J.M.J. Williams. Recent Res. Dev. Org. Bioorg. Chem. **3**, 47 (1999).
34. H. Stecher and K. Faber. Synthesis, 1 (1997).
35. R. Sturmer. Angew. Chem. Int. Ed. Engl. **36**, 1173 (1997).
36. S. Caddick and K. Jenkins. Chem. Soc. Rev. **25**, 447 (1996).
37. R.S. Ward. Tetrahedron: Asymmetry, **6**, 1475 (1995).
38. H.B. Kagan and J.C. Fiaud. *In* Topics in stereochemistry. Vol. 18. *Edited by* E.L. Eliel and S.H. Wilen. Wiley, New York. 1988. pp. 249–330.
39. J. Andraos. J. Chem. Educ. **76**, 1578 (1999) and refs. cited therein.
40. M. Kitamura, M. Tokunaga, and R. Noyori. Tetrahedron **49**, 1853 (1993).
41. R. Noyori, M. Tokunaga, and M. Kitamura. Bull. Chem. Soc. Jpn. **68**, 36 (1995).
42. For a typical example see: R.N. Ben and T. Durst. J. Org. Chem. **64**, 7700 (1999).
43. V.K. Balakrishnan. Schaum's outlines: graph theory. McGraw-Hill, New York. 1997.
44. E.L. King and C. Altman. J. Phys. Chem. **60**, 1375 (1956).
45. K.C. Chou. Eur. J. Biochem. **113**, 195 (1980).
46. K.C. Chou and S. Forsen. Biochem. J. **187**, 829 (1980).

47. K.C. Chou. J. Theor. Biol. **89**, 581 (1981).
48. K.C. Chou and L.W. Min. J. Theor. Biol. **91**, 637 (1981).
49. K.C. Chou and S. Forsen. Can. J. Chem. **59**, 737 (1981).
50. K.C. Chou. Biophys. Chem. **17**, 51 (1983).
51. K.C. Chou. J. Biol. Chem. **264**, 12074 (1989).
52. K.C. Chou. Biophys. Chem. **35**, 1 (1990).
53. K.C. Chou. J. Math. Chem. **12**, 97 (1993).
54. I.W. Althaus, J.J. Chou, A.J. Gonzales, M.R. Diebel, K.C. Chou, F.J. Kezdy, D.L. Romero, P.A. Aristoff, and W.G. Tarpley. J. Biol. Chem. **268**, 6119 (1993).
55. I.W. Althaus, A.J. Gonzales, J.J. Chou, M.R. Diebel, K.C. Chou, F.J. Kezdy, D.L. Romero, P.A. Aristoff, W.G. Tarpley, and F. Reusser. J. Biol. Chem. **268**, 14875 (1993).
56. I.W. Althaus, J.J. Chou, A.J. Gonzales, M.R. Diebel, K.C. Chou, F.J. Kezdy, D.L. Romero, P.A. Aristoff, W.G. Tarpley, and F. Reusser. Biochemistry, **32**, 6548 (1993).
57. I.W. Althaus, J.J. Chou, A.J. Gonzales, M.R. Diebel, K.C. Chou, F.J. Kezdy, D.L. Romero, R.C. Thomas, P.A. Aristoff, W.G. Tarpley, and F. Reusser. Biochem. Pharmacol. **47**, 2017 (1994).
58. S.X. Lin and K.E. Neet. J. Biol. Chem. **265**, 9670 (1990).
59. P. Kuzmic, K.Y. Ng, and T.D. Heath. Anal. Biochem. **200**, 68 (1992).
60. K.C. Chou, F.J. Kezdy, and F. Reusser. Anal. Biochem. **221**, 217 (1994).
61. G.P. Zhou and M.H. Deng. Biochem. J. **222**, 169 (1984).
62. G.E. Roberts and H. Kaufman. Table of Laplace transforms. Saunders, Philadelphia. 1966.
63. F. Oberhettinger and L. Badii. Tables of Laplace transforms. Springer, New York. 1973.
64. M. Healey. Tables of Laplace, Heaviside, Fourier and Z transforms. W. & R. Chambers, Edinburgh. 1967.
65. M.J. Gaunt, C.C.C. Johansson, A. McNally, and T. Vo Ngoc. Drug Discovery Today, **12**, 8 (2007).
66. G. Lelais and D.W.C. Macmillan. *In* New frontiers in asymmetric catalysis. *Edited by* K. Mikami and M. Lautens. Wiley, Hoboken, New Jersey. 2007. pp. 313–358.
67. R.M. de Figueiredo and M. Christmann. Eur. J. Org. Chem. 2575 (2007).
68. N. Marion, S. Diez-Gonzalez, and S.P. Nolan. Angew. Chem. Int. Ed. **46**, 2988 (2007).
69. S.B. Tsogoeva. Eur. J. Org. Chem. 1701 (2007).
70. G. Guillena, D.J. Ramon, and M. Yus. Tetrahedron: Asymmetry, **18**, 693 (2007).
71. D. Enders, C. Grondal, and M. Huettl. Angew. Chem. Int. Ed. **46**, 1570 (2007).
72. K. Maruoka, T. Ooi, and T. Kano. Chem. Commun. (Cambridge, U.K.), 1487 (2007).
73. S.V. Ley. *In* Asymmetric catalysis. *Edited by* M. Christmann and S. Braese. Wiley-VCH, Weinheim, Germany. 2007. pp. 201–206.
74. B. List. *In* Asymmetric catalysis. *Edited by* M. Christmann and S. Braese. Wiley-VCH, Weinheim, Germany. 2007. pp. 161–165.
75. D. Almasi, D.A. Alonso, and C. Najera. Tetrahedron: Asymmetry, **18**, 299 (2007).
76. M. Ikunaka. Org. Process Res. Dev. **11**, 495 (2007).
77. B. List. Chem. Commun. (Cambridge, U.K.), 819 (2006).
78. B. List and J.W. Yang. Science, **313**, 1584 (2006).
79. D. Tejedor, D. Gonzalez-Cruz, A. Santos-Exposito, J.J. Marrero-Tellado, P. de Armas, and F. Garcia-Tellado. Chem. Eur. J. **11**, 3502 (2005).
80. J. Saeyad and B. List. Org. Biomol. Chem. **3**, 719 (2005).
81. P.I. Dalko and L. Moisan. Angew. Chem. Int. Ed. **43**, 5138 (2004).
82. M.L. Clarke. Lett. Org. Chem. **1**, 292 (2004).
83. K.N. Houk and B. List. Acc. Chem. Res. **37**, 487 (2004).
84. P.R. Schreiner. Chem. Soc. Rev. **32**, 289 (2003).
85. N. Gathergood. Austr. J. Chem. **55**, 615 (2002).
86. P.I. Dalko and L. Moisan. Angew. Chem. Int. Ed. **40**, 3726 (2001).
87. S. Hoffmann, M. Nicoletti, and B. List. J. Am. Chem. Soc. **128**, 13074 (2006).
88. J.W. Yang, M.T.H. Fonseca, N. Vignola, B. List. Angew. Chem. Int. Ed. **44**, 108 (2005).
89. J. Franzen, M. Marigo, D. Fielenbach, T.C. Wabnitz, A. Kjaersgaard, and K.A. Jørgensen. J. Am. Chem. Soc. **127**, 18296 (2005).